

See discussions, stats, and author profiles for this publication at: <https://www.researchgate.net/publication/38087847>

Synthesis and Biological Evaluation of New Nanomolar Competitive Inhibitors of Helicobacter pylori Type II Dehydroquinase. Structural Details of the Role of the Aromatic Moieties w...

ARTICLE in JOURNAL OF MEDICINAL CHEMISTRY · NOVEMBER 2009

Impact Factor: 5.45 · DOI: 10.1021/jm9010466 · Source: PubMed

CITATIONS

12

READS

53

10 AUTHORS, INCLUDING:



José M Otero

University of Santiago de Compostela

49 PUBLICATIONS 376 CITATIONS

[SEE PROFILE](#)



Pablo Guardado-Calvo

Institut Pasteur

15 PUBLICATIONS 139 CITATIONS

[SEE PROFILE](#)



Antonio L. Llamas-Saiz

University of Santiago de Compostela

159 PUBLICATIONS 2,425 CITATIONS

[SEE PROFILE](#)



Mark Johan van Raaij

Spanish National Research Council

110 PUBLICATIONS 2,397 CITATIONS

[SEE PROFILE](#)

Synthesis and Biological Evaluation of New Nanomolar Competitive Inhibitors of *Helicobacter pylori* Type II Dehydroquinase. Structural Details of the Role of the Aromatic Moieties with Essential Residues^{†,‡}

Verónica F. V. Prazeres,[§] Lorena Tizón,[§] José M. Otero,^{||} Pablo Guardado-Calvo,^{||} Antonio L. Llamas-Saiz,[⊥] Mark J. van Raaij,^{||,#} Luis Castedo,[§] Heather Lamb,[○] Alastair R. Hawkins,[○] and Concepción González-Bello*,[§]

[§]Laboratorio de Química Orgánica (CSIC) y Departamento de Química Orgánica, Facultad de Química, Universidad de Santiago de Compostela, 15782 Santiago de Compostela, Spain, ^{||}Departamento de Bioquímica y Biología Molecular, Facultad de Farmacia, Universidad de Santiago de Compostela, 15782 Santiago de Compostela, Spain, [⊥]Unidad de Rayos X, Edificio CACTUS, Universidad de Santiago de Compostela, 15782 Santiago de Compostela, Spain, [#]Institut de Biología Molecular de Barcelona, Consejo Superior de Investigaciones Científicas (IBMB-CSIC), Parc Científic de Barcelona, Baldiri Reixach 10-12, E-08028 Barcelona, Spain, and [○]Institute of Cell and Molecular Biosciences, Medical School, University, Newcastle upon Tyne, Catherine Cookson Building, Framlington Place, Newcastle upon Tyne NE2 4HH, U.K.

Received July 14, 2009

The shikimic acid pathway is essential to many pathogens but absent in mammals. Enzymes in its pathway are therefore appropriate targets for the development of novel antibiotics. Dehydroquinase is the third enzyme of the pathway, catalyzing the reversible dehydration of 3-dehydroquinic acid to form 3-dehydroshikimic acid. Here we present the synthesis of novel inhibitors with high affinity for *Helicobacter pylori* type II dehydroquinase and efficient inhibition characteristics. The structure of *Helicobacter pylori* type II dehydroquinase in complex with the most potent inhibitor shows that the aromatic functional group interacts with the catalytic Tyr22 by π -stacking, expelling the Arg17 side chain, which is essential for catalysis, from the active site. The structure therefore explains the favorable properties of the inhibitor and will aid in design of improved antibiotics.

Introduction

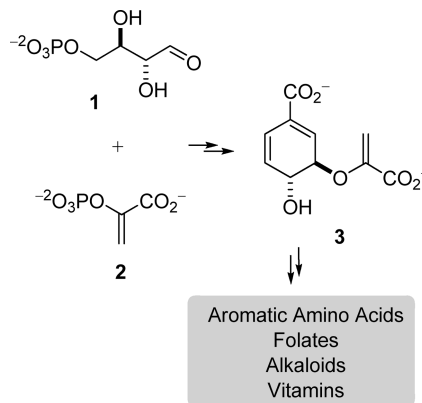
The capacity of antibiotics to cure infectious diseases that in the past were fatal, such as tuberculosis, pneumonia, bubonic plague, leprosy, and cholera, has ended in the false idea that antibiotics are miracle medicines with “powers”. However, in most of the cases, this belief exceeds their real pharmacology properties. The excessive use and in many cases misuse of antibiotics in medicine, veterinary, and agriculture has given rise to a fast increase of the prevalence of resistant microorganism to antibiotics.^{1,2} Therefore, the development of new agents that are able to overcome existing resistance mechanisms or that have novel mechanisms of action is much needed. The ulcer-causing *Helicobacter pylori* bacterium is a good example, with strains resistant to clarithromycin becoming more and more prevalent.^{3,4} Specifically, it has been estimated that the widespread of *H. pylori* resistance to clarithromycin is <5% for adults in northern Europe but as high as 20% in southern Europe.⁵ It is present in approximately 13% of patients in the U.S., but in selected regions such as Alaska, it has been reported to have rates as high as 30%.^{4,6} In addition, *H. pylori* infected persons are at increased risk for mucosa-associated lymphoid tissue lymphoma and gastric adenocarcinoma.⁷

[†]Coordinates and structure factors are available from the Protein Data Bank with accession code 2WKS.

[‡]Dedicated to Prof. Josep Font on the occasion of his 70th birthday.

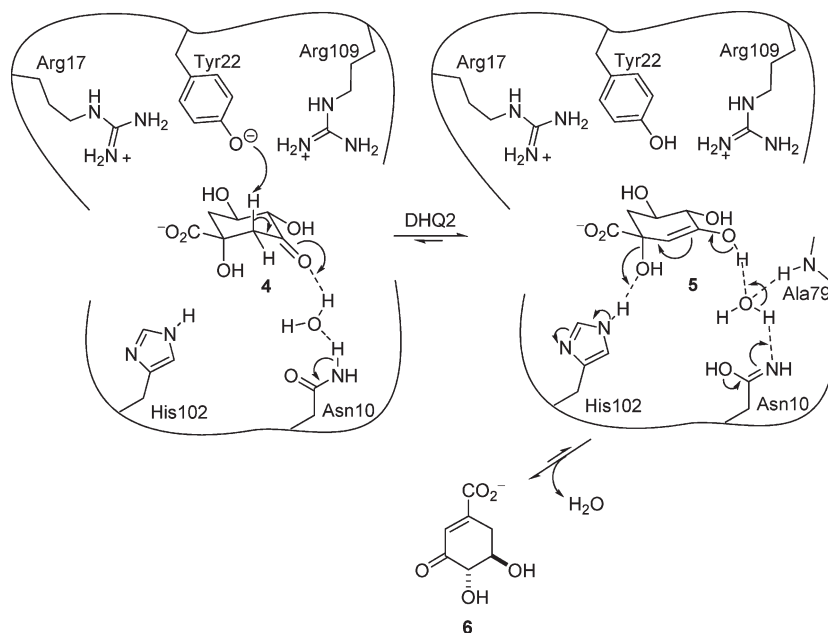
*To whom correspondence should be addressed. Phone: +34 981 563100 extension 14368. Fax: +34 981 595012. E-mail: concepcion.gonzalez.bello@usc.es.

Scheme 1. Shikimic Acid Pathway



In the past few years, our research group has been studying the possible development of new antibiotics whose action is based on the selective and effective inhibition of an essential route in bacteria, the shikimic acid pathway.⁸ This route consists of seven enzymes that catalyze the sequential conversion of erythrose 4-phosphate (**1**) and phosphoenol pyruvate (**2**) to chorismic acid (**3**), which is the precursor in the synthesis of aromatic compounds, including the aromatic amino acids L-phenylalanine, L-tyrosine, and L-tryptophan, folate cofactors, ubiquinone, and vitamins E and K (Scheme 1).^{9,10} This pathway is present in bacteria, fungi, and higher plants and has been discovered in apicomplexan parasites, *Plasmodium falciparum* (which are the cause of malaria),

Scheme 2. Proposed E1CB Mechanism for the Enzymatic Conversion of 3-Dehydroquinic Acid (**4**) to 3-Dehydroshikimic Acid (**6**) Catalyzed by DHQ2^a



^aThe reaction proceeds via the enol intermediate **5**. Relevant residues are indicated.

Toxoplasma gondii, and *Cryptosporidium parvum*.¹¹ The absence of the shikimate pathway in mammals, combined with its essential nature in certain microorganisms,^{12,13} makes it an attractive target for the development of new antimicrobial and antiparasitic agents.

Dehydroquinase (3-dehydroquinate dehydratase, DHQ,^a EC 4.2.1.10) is the third enzyme of the pathway, catalyzing the reversible dehydration of 3-dehydroquinic acid (**4**) to form 3-dehydroshikimic acid (**6**) (Scheme 2). Biochemical and genetic studies have shown that there are two different dehydroquinases, known as type I and type II, which do not have sequence homology and catalyze the same overall reaction but utilizing completely different mechanisms.^{14,15} The type I enzyme (DHQ1) is found in plants, fungi, archaeabacteria, and eubacterial species like *Escherichia coli* and *Salmonella typhi*.¹⁶ Type II dehydroquinase (DHQ2) is found in bacteria like *Streptomyces coelicolor*, *Mycobacterium tuberculosis*, and *Helicobacter pylori*.¹⁷

The proposed dehydration mechanism of DHQ2¹⁸ involves the abstraction of the pro-S hydrogen from C2 of the substrate, the 3-dehydroquinic acid (**4**), by Tyr22, for which the lower pK_a is the result of a basic environment formed by Arg17 and Arg109. Tyr22 and Arg17 have been identified by chemical modification and site-directed mutagenesis studies as being essential for enzyme activity.^{19,20} Both residues are on the flexible loop that closes over the active site upon substrate binding. The enol intermediate **5** is then generated, which is stabilized by a conserved molecule of water close to the carbonyl group side chain of Asn10, the carbonyl group of Pro9, and the main-chain amide of Ala79. The final step of

the mechanism is the elimination of the C1 hydroxyl group catalyzed by active-site His102.

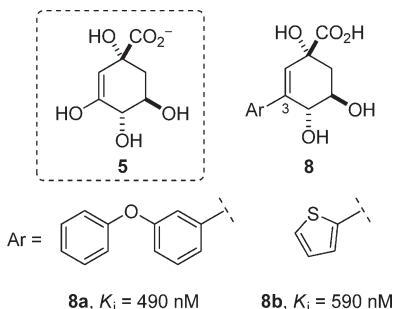
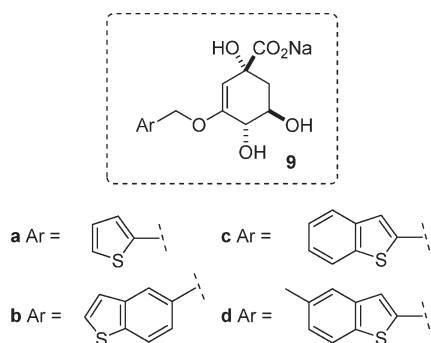
Recently, several enol mimics, compounds **8**, have been reported as competitive inhibitors of *H. pylori* type II dehydroquinase (DHQ2-Hp) (Figure 1).^{21,22} These compounds have an aromatic ring or a heteroaryl group on C3, which were incorporated to establish π -stacking interactions with essential Tyr22. The biaryl derivative **8a**²¹ and the 2-thienyl derivative **8b**²² proved to be the most potent ones, having a K_i of 490 and 540 nM, respectively. On the other hand, docking and NMR studies also suggested strong lipophilic interactions of the aromatic or the heterocyclic moieties with the enzyme residues Pro9, Asn10, Ile11, Gly78, and Ala79.²²

In the search for more potent inhibitors against this enzyme as potential antimicrobial agents, we report here the synthesis of four novel enol mimics, compounds **9**, with high affinity against *Helicobacter pylori* dehydroquinase (Figure 2). The crystal structure of DHQ2-Hp in complex with the enol mimic **9d** is also reported. The structure shows that the aromatic moiety indeed interacts with the catalytic Tyr22 by π -stacking, as designed. More importantly, it clarifies the possible interaction of the aromatic moiety with the essential Arg17. Inhibition studies of these compounds against DHQ2-Hp and docking studies using GOLD4.0 are also described.

Results

Synthesis of O-Alkylaryl Derivatives **9.** The synthesis of O-alkylaryl derivatives **9** was carried out by a three-step reaction sequence from our previously reported ketone **10**²³ (Scheme 3). The alkylaryl moieties of compounds **9** were introduced by O-alkylation of ketone **10**. Various bases (LDA, LHMDS, KHMDS), solvents (THF, DMF), leaving groups (tosylates, bromides, and iodides) and reaction temperatures were investigated. The best results were achieved using bromides as alkylating agents, KHMDS at -78°C or LHMDS at room temperature. Under these conditions a chromatographically separable mixture of the O-alkylated

^aAbbreviations: DHQ, 3-dehydroquinate dehydratase or dehydroquinase; DHQ1, type I dehydroquinase; DHQ2, type II dehydroquinase; DHQ2-Hp, type II dehydroquinase from *Helicobacter pylori*; PDB, Protein Data Bank; KHMDS, potassium hexamethyldisilazane; LHMDS, lithium hexamethyldisilazane; TBS, *tert*-butyldimethylsilyl; TBAF, tetrabutylammonium fluoride; DMF, *N,N*-dimethylformamide; THF, tetrahydrofuran; DTT, 1,4-dithiothreitol; Tris, tris(hydroxymethyl)aminomethane.

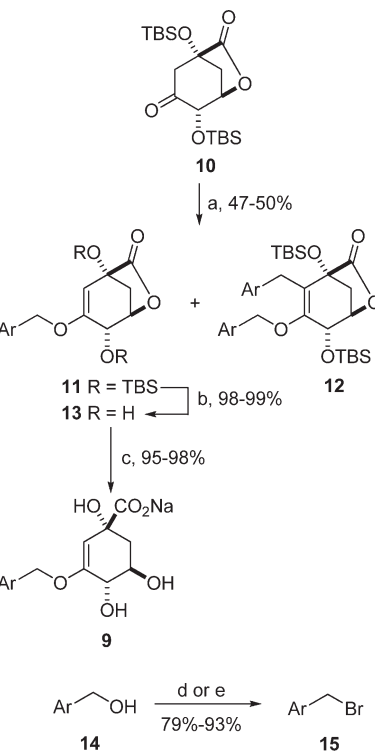
**Figure 1.** Enol mimics as competitive inhibitors of DHQ2-Hp.**Figure 2.** New enol mimics.

11 and the dialkylated products **12** was obtained in moderate yield. The required bromides **15** were prepared by bromination of the corresponding commercially available alcohols **14**. Finally, deprotection of the TBS groups with TBAF followed by basic hydrolysis of the corresponding lactone **13** gave the desired enol mimics **9**.

Inhibition Assay Results. Compounds **9** were assayed in the presence of 3-dehydroquinic acid (**4**) for their inhibitory properties against DHQ2-Hp. The inhibition data, as obtained from Dixon plots ($1/v$ vs $[I]$),²⁴ are summarized in Table 1. The UV spectrophotometric assay was used to measure the initial rate of product formation, detecting the enone–carboxylate chromophore at 234 nm in 3-dehydroshikimic acid (**6**).

All the compounds were shown to be reversible competitive inhibitors of DHQ2-Hp, proving to have (with the exception of thiophene **9a**) higher affinity than the best previously reported competitive inhibitors, compounds **8a**²¹ and **8b**.²² Substitution of the thiophenyl ring by a benzothiophenyl one improves more than 5 times the inhibition potency of the corresponding analogues. There is a slight difference in K_i among 5-benzothiophenyl **9b** ($K_i = 166 \text{ nM}$) and 2-benzothiophenyl derivatives **9c** ($K_i = 132 \text{ nM}$), but almost no affinity changes were found with the incorporation of a methyl group on the benzothiophene motif. The methylbenzothiophene **9d** proved to be the most potent of the series with a K_i of 130 nM.

Structural Studies. To obtain structural information on the binding mechanism of these inhibitors, we cocrystallized the most potent competitive inhibitor of the series, methylbenzothiophene **9d**, with DHQ2-Hp. Data were collected from cryocooled crystals using synchrotron radiation and processed (Table 2). The structure was solved by molecular replacement, using the crystal structure of dehydroquinase bound to citrate²⁵ as a search model. Difference density analysis showed the two structures are virtually identical

Scheme 3^a

- a** Ar = 2-thienyl
b Ar = benzo[b]thiophen-5-yl
c Ar = benzo[b]thiophen-2-yl
d Ar = 5-methylbenzo[b]thiophen-2-yl

^a Reagents and conditions: (a) (1) KHMDS, DMF, -78°C or LHMDS, DMF, room temp, (2) **15**; (b) TBAF, THF, 0°C ; (c) NaOH, THF, room temp; (d) PPh_3 , CBr_4 , DCM, room temp; (e) PBr_3 , Py, 0°C to room temp.

Table 1. K_i (nM) of Compounds **9** against DHQ2-Hp^a

| Compound | Ar | K_i |
|-----------|----|--------------|
| 9a | | 920 ± 90 |
| 9b | | 166 ± 15 |
| 9c | | 132 ± 13 |
| 9d | | 130 ± 13 |

^a 50 mM Tris-HCl, pH 7.0, 25°C .

(1.0 Å root-mean-square difference after superimposition), but amino acids 15–23 changed conformation upon inhibitor binding. In the same region, calculated maps showed clear electron density for the inhibitor molecule, which was modeled at full occupancy in each of the six crystallographically independent monomers (Figure 3; see also Supporting Information). Parallel refinements were performed with the benzothiophene ring in each of two orientations, rotated

Table 2. Crystallographic Data Collection and Refinement Statistics of DHQ2-Hp Complex with Inhibitor **9d**

| parameter ^a | |
|---|--|
| space group | <i>I</i> 4 ₁ |
| cell parameters (Å) | <i>a</i> = <i>b</i> = 157.85, ^b <i>c</i> = 99.78 |
| wavelength (Å) | 0.8150 |
| detector | MAR555 flat panel detector |
| crystal-to-detector distance (mm) | 350.0 |
| observed reflections ^c | 25 927 (3794) ^d |
| resolution range (Å) | 31.0–2.95 (3.11–2.95) |
| Wilson B (Å ²) | 74.7 |
| multiplicity | 6.5 (6.5) |
| completeness | 0.999 (0.999) |
| <i>R</i> _{merge} | 0.103 (0.394) |
| Refinement ^e | |
| reflections used in refinement ^c | 24653 (3579) |
| reflections used for <i>R</i> _{free} | 1198 (155) |
| resolution range (Å) | 20.0–2.95 (3.11–2.95) |
| <i>R</i> factor ^f | 0.206 (0.29) |
| <i>R</i> _{free} ^g | 0.236 (0.31) |
| rmsd (bonds (Å)/angles (deg)) | 0.014/1.5 |
| Final Model | |
| protein/inhibitor/water atoms | 7092/144/21 |
| average B protein (Å ²)/ inhibitor (Å ²)/ water (Å ²) | 52.2/58.2/37.0 |
| Ramachandran statistics ^h (%) | 93.5/100.0 |

^a Results from MOSFLM (ref 22). ^b 1 Å is 0.1 nm. ^c No σ cutoff or other restrictions were used for inclusion of reflections. ^d Values in parentheses are for the highest resolution bin, where applicable. ^e Results from REFMAC (ref 33). ^f $R = \sum ||F_{\text{obs}}(\text{hkl})| - |F_{\text{calc}}(\text{hkl})|| / \sum |F_{\text{obs}}(\text{hkl})|$. ^g According to ref 31. ^h According to the program MOLPROBITY (ref 34). The percentages indicated are for residues in favored and total allowed regions, respectively.

180° around the bond that connects it to the CH₂ group. Refinement parameters were slightly better for the orientation shown (*R*-factor 0.1% improved, *R*_{free} of 0.4%), and the maps also suggested the more electron dense sulfur atom to be located on the side of the ring as shown in Figure 3 (see also Supporting Information). However, at the resolution of the studies reported, we cannot exclude the presence of a mixture of the two conformations. After refinement, temperature factors for the carbasugar moiety were 30–50 Å², comparable to those of surrounding amino acids (around 35 Å²). The benzothiophene ring system has higher temperature factors (around 75 Å²) and is more poorly ordered; correspondingly, electron density is weaker for this part of the inhibitor (Figure 3). Surrounding amino acids (loop 15–23) have similar temperature factors. Thus, this loop, in the presence of inhibitor, is conformationally flexible. Despite the disorder, the structure shows that the benzothiophene moiety interacts with Tyr22 by π-stacking, expelling Arg17 from the active site (Figure 4). The benzothiophene ring system takes the place of the side chain of Arg17 in the active site, an essential residue for catalysis. This crystal structure also shows that the benzothiophene moiety is in close contact

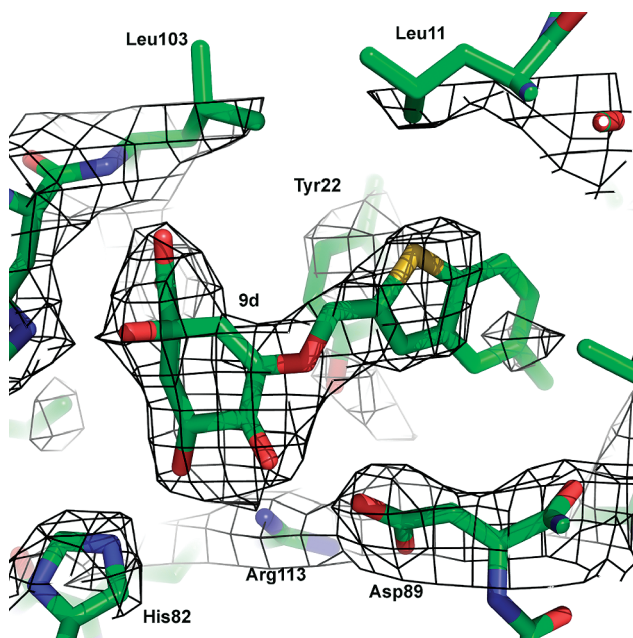


Figure 3. Electron density for inhibitor **9d** in monomer A of the crystal structure of DHQ2-Hp. From the model obtained by molecular replacement, amino acids 15–23 of each of the six monomers were removed and refinement was performed with tight noncrystallographic restraints to obtain unbiased density for the inhibitor molecules and other model changes. A maximum-likelihood weighted $2F_{\text{o}} - F_{\text{c}}$ map³³ contoured at 1σ is shown up to 3 Å around the inhibitor molecules. Onto the map, the final model, as deposited into the database, including inhibitor molecules, is superposed.

with side chain atoms of Met13, Leu14, and Pro19, establishing important lipophilic interactions with this part of the active site (Figure 5c). In addition, hydrogen H-2 of the cyclohexene ring and the methylene group of the inhibitor side chain are in close contact with the side chain of Leu11. The methyl group of the benzothiophene ring is close to the side chain of Leu93 and Met92 of the neighbor subunit of the DHQ2-Hp.

Docking Studies. In order to rationalize the inhibition observations noted above, docking studies were carried out using GOLD 4.0²⁶ and the enzyme geometries found in crystal of DHQ2-Hp binding inhibitor **9d**. A good correlation between the experimental inhibition data and the scored solution of ligands **9a–c** were found. Ligands **9a–c** docked with its cyclohexene ring and carboxyl group occupying approximately the same locations as those of the ligand **9d** in the crystal structure. The docking results also showed that the ligands side chains are in a similar orientation to binding inhibitor **9d** (Figure 5). However, important differences were found in the space occupied by the side chain of the ligands and therefore in their proximity to side chain atoms of Met13, Leu14, and Pro19 of the active site and Leu93 and Met92 of the neighbor subunit of the enzyme. It can be seen from Figure 5c that in the proposed binding mode of ligand **9a**, its side chain occupies only part of the benzothiophene pocket. In this case, the flexible loop including Arg17 is probably closer to the active site than in the crystal structure of DHQ2-Hp/**9d** complex. Docking studies also predict a stronger affinity of the 2-benzothiophene derivative **9c** than its 5-isomer, derivative **9b**. This fact could be a result of the balance between the differences in the strength of the π-stacking interactions between the benzothiophene moiety

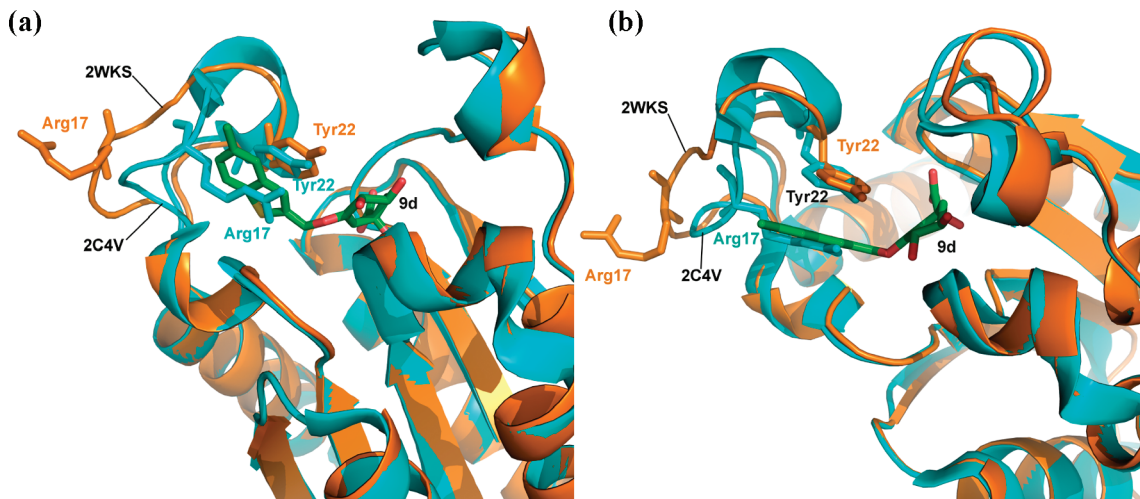


Figure 4. Superposition of DHQ2-Hp structure with (orange) and without inhibitor **9d** (light-blue). The structure without inhibitor is PDB entry 2C4V. Two different orientations are shown in panels a and b, zoomed-in on the active site of monomer A. While Tyr22 only slightly adjusts its position, the side chain of Arg17 flips out of the active site as a result of the benzothiophene ring system taking its place. Arg109 (not shown) does not change position significantly.

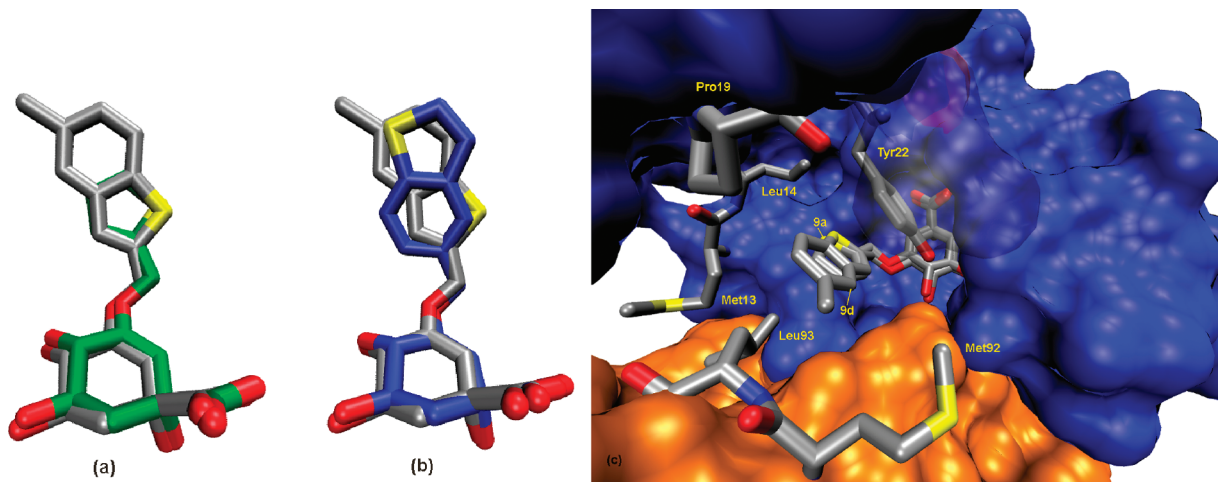


Figure 5. Comparison of the position of inhibitor **9d** in the enzyme–inhibitor crystal structure of DHQ2-Hp with the docking results of the highest score solution of ligands: (a) **9a** (green); (b) **9b** (blue); (c) selected view of GOLD-predicted binding of ligand **9a**.

and the aromatic ring of Tyr22 and the lipophilic interactions with the above-mentioned residues.

Conclusions and Final Remarks

Four new enol mimics, compounds **9**, were synthesized and tested as inhibitors of DHQ2-Hp, the third enzyme of the shikimic acid pathway. All of these compounds proved to be reversible competitive inhibitors of this enzyme. With the exception of 2-thienyl derivative **9a**, all the reported compounds proved to be more potent than the best previously reported compounds for this enzyme, having K_i ranging from 130 to 166 nM, representing an improved affinity of almost 4-fold. The 2-benzothiophenyl derivatives **9c** and **9d** proved to be the most potent ones with K_i of 132 and 130 nM, respectively.

The most potent competitive inhibitor of the series, methylbenzothiophene **9d** was cocrystallized with DHQ2-Hp, and its structure has been solved at 2.95 Å. This crystal structure proves that the benzothiophene moiety of **9d** interacts with Tyr22 by π -stacking as designed, a residue that has been

identified to act as the base in the enzymatic mechanism. More importantly, this structure clarifies the possible interaction of the aromatic moiety with Arg17, a residue also essential for catalysis that is responsible, together with Arg109, for the low pK_a of the Tyr22. The competitive inhibitor **9d** expels Arg17 from the active site, and the benzothiophene moiety occupies the place of Arg17 side chain. This fact is probably due to important lipophilic interactions that the benzothiophene moiety can establish with the side chain residues of this part of the active site, in particular Met13, Leu14, Pro19, and Leu11, and also with the side chain of Leu93 and Met92 of the neighbor subunit.

Therefore, we have shown that the high affinity of this new enol mimics is due to two effects with essential residues for the catalysis, i.e., a π -stacking interaction between the benzothiophene ring and the aromatic ring of Tyr22 and, on the other hand, the expulsion of the Arg17 from the active site. The availability of this structure now opens the possibility for the structural design of the next generation of competitive inhibitors against this enzyme, which is in progress.

Experimental Section

General Procedures. All starting materials and reagents were commercially available and used without further purification. FT-IR spectra were recorded as NaCl plates, or KBr discs. $[\alpha]_D^{20}$ values are given in 10^{-1} deg $\text{cm}^2 \text{ g}^{-1}$. ^1H NMR spectra (250, 300, 400, and 500 MHz) and ^{13}C NMR spectra (63, 75, 100, and 125 MHz) were measured in deuterated solvents. J values are given in hertz. NMR assignments were made by a combination of 1D, COSY, and DEPT-135 experiments. Purities of compounds **9** were determined by a combination of ^1H NMR and reverse-phase HPLC and were found to be $> 95\%$.

(2-Bromomethyl)thiophene (15a). A solution of thien-2-ylmethanol (**14a**) (1 mL, 10.55 mmol), phosphorus tribromide (1.5 mL, 15.83 mmol), and three drops of dry pyridine in dry dichloromethane (40 mL), under argon and 0 °C, was stirred for 1 h. During this period, the reaction mixture was allowed to reach room temperature. Water was then added, and the organic phase was separated. The aqueous layer was extracted with dichloromethane ($\times 2$). All the combined organic extracts were washed with saturated sodium bicarbonate, dried (anhydrous Na_2SO_4), filtered, and concentrated under reduced pressure to afford bromide **15a** (1.5 g, 80%) as a light-yellow oil. ^1H NMR (250 MHz, CDCl_3) δ 7.73 (dd, 1H, $J = 5.0$ and 1.0 Hz, H-5), 7.52 (d, 1H, $J = 3.0$ Hz, H-3), 7.35 (dd, 1H, $J = 5.0$ and 3.0 Hz, H-4), and 5.16 (s, 2H, CH_2Br) ppm. ^{13}C NMR (63 MHz, CDCl_3) δ 141.9 (C), 131.8 (CH), 128.4 (CH), 128.2 (CH), and 26.7 (CH₂) ppm.

(5-Bromomethyl)benzo[b]thiophene (15b). To a stirred solution of benzo[b]thiophen-5-ylmethanol (**14b**) (100 mg, 0.61 mmol) in dry dichloromethane (15 mL) and under argon, PPh_3 (290 mg, 1.09 mmol) and then CBr_4 (240 mg, 0.73 mmol) were added. After the mixture was stirred for 1 h, diethyl ether was added and the resulting precipitate was filtered and washed with diethyl ether. The solvents were removed under reduced pressure and the crude residue was purified by flash chromatography, eluting with (10:90) diethyl ether/hexanes to afford bromide **15b** (129 mg, 93%) as a white amorphous solid. ^1H NMR (250 MHz, CDCl_3) δ 7.86 (m, 2H, 2 \times ArH), 7.49 (d, 1H, $J = 5.5$ Hz, ArH), 7.39 (d, 1H, $J = 8.7$ Hz, ArH), 7.33 (d, 1H, $J = 5.5$ Hz, ArH), and 4.66 (s, 2H, CH_2O) ppm. ^{13}C NMR (63 MHz, CDCl_3) δ 139.7 (C), 139.7 (C), 133.8 (C), 127.4 (CH), 125.2 (CH), 123.9 (CH), 123.7 (CH), 122.8 (CH), and 34.1 (CH₂) ppm. MS (CI) m/z (%) 227 and 229 (MH^+). HRMS calcd for $\text{C}_{9}\text{H}_{8}\text{S}^{79}\text{Br} (\text{MH}^+)$: 226.9530; found, 226.9532.

(2-Bromomethyl)benzo[b]thiophene (15c). The reaction was carried out as for bromide **15b** by using benzo[b]thiophen-2-ylmethanol (**14c**) (1.0 g, 6.09 mmol) as starting material, 2.88 g of PPh_3 , 2.42 g of CBr_4 , and 152 mL of dichloromethane. Yield: 1.08 g (79%). White amorphous solid. ^1H NMR (250 MHz, CDCl_3) δ 7.82–7.70 (m, 2H, 2 \times ArH), 7.40–7.33 (m, 3H, 3 \times ArH), and 4.80 (s, 2H, CH_2) ppm. ^{13}C NMR (63 MHz, CDCl_3) δ 141.0 (C), 140.5 (C), 139.1 (C), 125.0 (C), 124.6 (CH), 124.5 (CH), 123.8 (CH), 122.4 (CH), and 27.3 (CH₂) ppm.

2-(Bromomethyl)-5-methylbenzo[b]thiophene (15d). The reaction was carried out as for bromide **15b** by using (5-methylbenzo[b]thiophen-2-yl)methanol (**14d**) (50 mg, 0.28 mmol), 131 mg of PPh_3 , 113 mg of CBr_4 , and 7.0 mL of dichloromethane. Yield: 59 mg (88%). White amorphous solid. Mp 98–101 °C. ^1H NMR (250 MHz, CDCl_3) δ 7.67 (d, 1H, $J = 8.3$ Hz, H-4), 7.53 (br s, 1H, H-7), 7.25 (s, 1H, H-3), 7.18 (d, 1H, $J = 8.3$ and 0.8 Hz, H-5), 4.79 (s, 2H, CH_2), and 2.47 (s, 3H, CH_3) ppm. ^{13}C NMR (63 MHz, CDCl_3) δ 141.0 (C), 139.5 (C), 137.7 (C), 134.3 (C), 126.7 (CH), 124.2 (CH), 123.7 (CH), 122.0 (CH), 27.5 (CH₂), and 21.3 (CH₃) ppm.

(1R,4S,5R)-1,4-Di(tert-butyldimethylsilyloxy)-3-(thien-3-yl)methoxycyclohex-2-en-1,5-carbolactone (11a) and (1R,4S,5R)-1,4-di(tert-butyldimethylsilyloxy)-3-(thien-3-yl)methoxy-2-(thien-3-yl)methylcyclohex-2-en-1,5-carbolactone (12a). A flame-dried round-bottom flask was charged with KHMDS (3 mL, 1.5 mmol, 0.5 M in

toluene) and dry DMF (1.5 mL) under inert atmosphere. The resultant solution was cooled to -78 °C, and then a solution of ketone **10**²³ (300 mg, 0.75 mmol) in a 1:1 mixture of DMF and toluene (7.5 mL), both dry, was added. After the mixture was stirred for 30 min, a solution of 2-(bromomethyl)thiophene (**15a**) (265 mg, 1.50 mmol) in a 3:2 mixture of DMF and toluene (6.25 mL), both dry, was added. After 45 min, the reaction mixture was diluted successively with diethyl ether and water. The organic phase was separated, and the aqueous layer was extracted with diethyl ether ($\times 2$). All the combined organic extracts were dried (anhydrous Na_2SO_4), filtered, and evaporated under reduced pressure. The obtained residue was purified by flash chromatography, eluting with diethyl ether–hexanes [(1) 0:100, (2) 5:95] to afford *O*-alkyl derivative **11a** (67 mg, 18%) and dialkyl derivative **12a** (153 mg, 35%).

Data for 11a. White solid. Mp: 65–67 °C. $[\alpha]_D^{20} -133^\circ$ (*c* 1.2, CHCl_3). ^1H NMR (250 MHz, CDCl_3) δ 7.31 (dd, 1H, $J = 5.0$ and 1.2 Hz, ArH), 7.03 (d, 1H, $J = 2.8$ Hz, ArH), 6.98 (dd, 1H, $J = 5.0$ and 3.8 Hz, ArH), 5.01 (s, 1H, H-2), 4.90 (d, 1H, $J = 11.5$ Hz, CHHAr), 4.84 (d, 1H, $J = 11.5$ Hz, CHHAr), 4.47 (dd, 1H, $J = 5.2$ and 3.5 Hz, H-5), 4.14 (d, 1H, $J = 3.5$ Hz, H-4), 2.40 (d, 1H, $J = 10.5$ Hz, H-6_{ax}), 2.33 (dd, 1H, $J = 10.5$ and 5.2 Hz, H-6_{eq}), 0.93 (s, 9H, $\text{C}(\text{CH}_3)_3$), 0.87 (s, 9H, $\text{C}(\text{CH}_3)_3$), 0.19 (s, 3H, SiCH_3), 0.15 (s, 3H, SiCH_3), 0.08 (s, 3H, SiCH_3), and 0.05 (s, 3H, SiCH_3) ppm. ^{13}C NMR (63 MHz, CDCl_3) δ 176.1 (C), 153.2 (C), 137.7 (C), 127.1 (CH), 126.5 (CH), 126.3 (CH), 104.8 (CH), 75.2 (CH), 73.6 (C), 67.3 (CH), 64.3 (CH₂), 37.9 (CH₂), 25.6 (C(CH_3)₃), 25.5 (C(CH_3)₃), 18.0 (2 \times C(CH_3)₃), -3.1 (2 \times CH₃), -4.6 (CH₃), and -5.3 (CH₃) ppm. IR (KBr): 1801 (C=O) cm^{-1} . MS (CI) m/z (%) 497 (MH^+). HRMS calcd for $\text{C}_{24}\text{H}_{41}\text{O}_5\text{SSi}_2 (\text{MH}^+)$: 497.2213; found, 497.2214.

Data for 12a. Yellow oil. $[\alpha]_D^{20} -127^\circ$ (*c* 1.0, CHCl_3). ^1H NMR (300 MHz, CDCl_3) δ 7.29 (d, 1H, $J = 4.2$ Hz, ArH), 7.06 (d, 1H, $J = 4.5$ Hz, ArH), 6.92 (m, 3H, 3 \times ArH), 6.77 (s, 1H, ArH), 4.96 (s, 2H, CH_2O), 4.54 (m, 1H, H-5), 4.42 (br s, 1H, H-4), 3.79 (d, 1H, $J = 15.0$ Hz, CHHAr), 3.69 (d, 1H, $J = 15.0$ Hz, CHHAr), 2.53 (d, 1H, $J = 10.8$ Hz, H-6_{ax}), 2.41 (dd, 1H, $J = 10.8$ and 5.7 Hz, H-6_{eq}), 0.95 (s, 9H, $\text{C}(\text{CH}_3)_3$), 0.80 (s, 9H, $\text{C}(\text{CH}_3)_3$), 0.20 (s, 3H, CH_3), 0.18 (s, 3H, CH_3), 0.17 (s, 3H, CH_3), and 0.06 (s, 3H, CH_3) ppm. ^{13}C NMR (75 MHz, CDCl_3) δ 175.3 (C), 148.2 (C), 142.8 (C), 138.8 (C), 129.7 (C), 126.9 (CH), 126.7 (CH), 126.4 (CH), 126.3 (CH), 124.5 (CH), 122.8 (CH), 74.6 (CH + C), 67.5 (CH₂), 67.2 (CH), 37.5 (CH₂), 25.7 (C(CH_3)₃), 25.5 (C(CH_3)₃), 24.7 (CH₂), 18.1 (C(CH_3)₃), 18.0 (C(CH_3)₃), -3.3 (CH₃), -3.5 (CH₃), and -4.5 (2 \times CH₃) ppm. IR (film): 1799 (C=O) cm^{-1} . MS (CI) m/z (%) 593 (MH^+). HRMS calcd for $\text{C}_{29}\text{H}_{45}\text{O}_5\text{S}_2\text{Si}_2 (\text{MH}^+)$: 593.2247; found, 593.2248.

(1R,4S,5R)-1,4-Di(tert-butyldimethylsilyloxy)-3-(benzo[b]thiophen-5-yl)methoxycyclohex-2-en-1,5-carbolactone (11b) and (1R,4S,5R)-1,4-Di(tert-butyldimethylsilyloxy)-3-(benzo[b]thiophen-5-yl)methoxy-2-(benzo[b]thiophen-5-yl)methylcyclohex-2-en-1,5-carbolactone (12b). The reaction was carried out as for compounds **11a** and **12a** by using 500 mg of ketone **10** and 570 mg of (5-bromomethyl)benzo[b]thiophene (**15b**) as starting materials. Yield: 173 mg (25%) of *O*-alkyl derivative **11b** and 237 mg (27%) of dialkyl derivative **12b**.

Data for 11b. Colorless oil. $[\alpha]_D^{20} -108^\circ$ (*c* 1.2, CHCl_3). ^1H NMR (250 MHz, CDCl_3) δ 7.79 (d, 1H, $J = 8.2$ Hz, ArH), 7.72 (s, 1H, ArH), 7.39 (d, 1H, $J = 5.2$ Hz, ArH), 7.24 (m, 2H, 2 \times ArH), 4.97 (s, 1H, H-2), 4.82 (d, 1H, $J = 11.2$ Hz, CHHO), 4.74 (d, 1H, $J = 11.2$ Hz, CHHO), 4.43 (dd, 1H, $J = 5.0$ and 3.5 Hz, H-5), 4.13 (d, 1H, $J = 3.5$ Hz, H-4), 2.35 (d, 1H, $J = 10.5$ Hz, H-6_{ax}), 2.28 (m, 1H, H-6_{eq}), 0.87 (s, 9H, $\text{C}(\text{CH}_3)_3$), 0.82 (s, 9H, $\text{C}(\text{CH}_3)_3$), 0.09 (s, 3H, SiCH_3), 0.04 (s, 3H, SiCH_3), 0.02 (s, 3H, SiCH_3), and -0.01 (s, 3H, SiCH_3) ppm. ^{13}C NMR (63 MHz, CDCl_3) δ 176.1 (C), 153.4 (C), 139.6 (C), 139.3 (C), 131.9 (C), 127.0 (CH), 124.0 (CH), 123.7 (CH), 122.8 (CH), 122.4 (CH), 104.9 (CH), 75.2 (C), 73.7 (C), 69.6 (CH₂), 67.4 (CH), 38.0 (CH₂), 25.6 (C(CH_3)₃), 25.5 (C(CH_3)₃), 18.0 (C(CH_3)₃), 17.9 (C(CH_3)₃), -3.2 (2 \times SiCH₃), -4.6 (SiCH₃), and -5.2 (SiCH₃)

ppm. IR (film): 1801 ($\text{C}=\text{O}$) cm^{-1} . MS (CI) m/z (%) 547 (MH^+). HRMS calcd for $\text{C}_{28}\text{H}_{43}\text{O}_5\text{SSi}_2$ (MH^+): 547.2370; found, 547.2375.

Data for 12b. Colorless oil. $[\alpha]_D^{20} -87^\circ$ (c 1.7, CHCl_3). ^1H NMR (250 MHz, CDCl_3) δ 7.77 (d, 1H, $J = 8.5$ Hz, ArH), 7.69 (d, 1H, $J = 8.5$ Hz, ArH), 7.57 (s, 1H, ArH), 7.55 (s, 1H, ArH), 7.43 (d, 1H, $J = 5.5$ Hz, ArH), 7.36 (d, 1H, $J = 5.5$ Hz, ArH), 7.23–7.12 (m, 4H, $4 \times$ ArH), 4.89 (d, 1H, $J = 11.2$ Hz, OCHH), 4.77 (d, 1H, $J = 11.2$ Hz, OCHH), 4.53 (dd, 1H, $J = 5.5$ and 3.5 Hz, H-5), 4.48 (d, 1H, $J = 3.5$ Hz, H-4), 3.81 (d, 1H, $J = 15.0$ Hz, CHHAr), 3.66 (d, 1H, $J = 15.0$ Hz, CHHAr), 2.56 (d, 1H, $J = 10.8$ Hz, H-6_{ax}), 2.44 (dd, 1H, $J = 10.8$ and 5.5 Hz, H-6_{eq}), 0.95 (s, 9H, $\text{C}(\text{CH}_3)_3$), 0.73 (s, 9H, $\text{C}(\text{CH}_3)_3$), 0.17 (s, 3H, SiCH₃), 0.16 (s, 3H, SiCH₃), 0.13 (s, 3H, SiCH₃), and 0.03 (s, 3H, SiCH₃) ppm. ^{13}C NMR (63 MHz, CDCl_3) δ 175.6 (C), 148.7 (C), 139.6 (C), 139.5 (C), 136.9 (C), 136.1 (C), 132.9 (C), 129.2 (C), 128.5 (C), 126.7 (CH), 125.9 (CH), 125.3 (CH), 123.8 (CH), 123.6 (CH), 123.5 (CH), 123.1 (CH), 122.3 (CH), 122.2 (CH), 121.7 (CH), 74.9 (C), 72.6 (CH₂), 67.1 (CH), 37.6 (CH₂), 29.9 (CH₂), 25.6 ($\text{C}(\text{CH}_3)_3$), 25.4 ($\text{C}(\text{CH}_3)_3$), 17.9 ($2 \times \text{C}(\text{CH}_3)_3$), –3.4 (SiCH₃), –3.6 (SiCH₃), and –4.5 ($2 \times \text{SiCH}_3$) ppm. IR (film): 1799 ($\text{C}=\text{O}$) cm^{-1} . MS (CI) m/z (%) 693 (MH^+). HRMS calcd for $\text{C}_{37}\text{H}_{49}\text{O}_5\text{S}_2\text{Si}_2$ (MH^+): 693.2560; found, 693.2464.

(**1R,4S,5R**)-**1,4-Di(tert-butylidemethylsilyloxy)-3-(benzo[b]thiophen-2-yl)methoxycyclohexan-1,5-carbolactone (11c)** and (**1R,4S,5R**)-**1,4-Di(tert-butylidemethylsilyloxy)-2-(benzo[b]thiophen-2-yl)methyl-3-(benzo[b]thiophen-2-yl)methoxycyclohexan-1,5-carbolactone (12c).** A flame-dried round-bottom flask under inert atmosphere was charged with ketone **10** (250 mg, 0.63 mmol) and then dissolved in dry DMF (17 mL). The resultant solution was treated with LHMDS (1.3 mL, 1.26 mmol, 1.0 M in THF). After the mixture was stirred for 20 min, a solution of (2-bromomethyl)benzo[b]thiophene (**15c**) (215 mg, 0.95 mmol) in dry DMF (1.6 mL) was added. After 30 min, the reaction mixture was diluted successively with diethyl ether and water. The organic phase was separated, and the aqueous layer was extracted three times with diethyl ether. All combined organic extracts were dried (anhydrous Na_2SO_4), filtered, and evaporated under reduced pressure. The obtained residue was purified by flash chromatography, eluting with diethyl ether–hexanes (5:95) to afford *O*-alkyl derivative **11c** (63 mg, 18%) and dialkyl derivatives **12c** (128 mg, 29%), both as light-yellow oils.

Data for 11c. $[\alpha]_D^{20} -103.3^\circ$ (c 2.1, CHCl_3). ^1H NMR (250 MHz, CDCl_3) δ 7.86–7.79 (m, 1H, ArH), 7.78–7.72 (m, 1H, ArH), 7.35 (m, 2H, $2 \times$ ArH), 7.25 (m, 1H, ArH), 5.06 (s, 1H, H-2), 5.01 (d, 1H, $J = 12.0$ Hz, CHHAr), 4.95 (d, 1H, $J = 12.0$ Hz, CHHAr), 4.49 (dd, 1H, $J = 5.5$ and 3.5 Hz, H-5), 4.19 (d, 1H, $J = 3.5$ Hz, H-6_{ax}), 2.42 (d, 1H, $J = 10.8$ Hz, H-6_{ax}), 2.34 (ddd, 1H, $J = 10.8$, 5.5, and 1.1 Hz, H-6_{ax}), 0.93 (s, 9H, $\text{C}(\text{CH}_3)_3$), 0.89 (s, 9H, $\text{C}(\text{CH}_3)_3$), 0.17 (s, 3H, SiCH₃), 0.13 (s, 3H, SiCH₃), 0.11 (s, 3H, SiCH₃), and 0.10 (s, 3H, SiCH₃) ppm. ^{13}C NMR (63 MHz, CDCl_3) δ 176.1 (C), 153.2 (C), 140.3 (C), 139.1 (C), 138.9 (C), 124.5 (CH), 124.3 (CH), 123.6 (CH), 123.3 (CH), 122.4 (CH), 105.3 (CH), 75.3 (CH), 73.7 (C), 67.4 (CH), 65.2 (CH₂), 38.0 (CH₂), 25.7 ($\text{C}(\text{CH}_3)_3$), 25.6 ($\text{C}(\text{CH}_3)_3$), 18.1 ($\text{C}(\text{CH}_3)_3$), 18.0 ($\text{C}(\text{CH}_3)_3$), –3.1 ($2 \times \text{SiCH}_3$), –4.4 (SiCH₃), and –5.1 (SiCH₃) ppm. IR (film): 1803 ($\text{C}=\text{O}$) cm^{-1} . MS (CI) m/z (%) 547 (MH^+). HRMS calcd for $\text{C}_{28}\text{H}_{43}\text{O}_5\text{SSi}_2$ (MH^+): 547.2370; found, 547.2372.

Data for 12c. $[\alpha]_D^{20} -148.6^\circ$ (c 1.0, CHCl_3). ^1H NMR (250 MHz, CDCl_3) δ 7.82–7.67 (m, 3H, $3 \times$ ArH), 7.61 (m, 1H, ArH), 7.38–7.20 (m, 4H, $4 \times$ ArH), 7.06 (s, 1H, ArH), 7.00 (s, 1H, ArH), 5.07 (s, 2H, OCH₂), 4.60 (dd, 1H, $J = 5.5$ and 3.3 Hz, H-5), 4.50 (d, 1H, $J = 3.3$ Hz, H-4), 3.98 (d, 1H, $J = 15.5$ Hz, CHHAr), 3.83 (d, 1H, $J = 15.5$ Hz, CHHAr), 2.60 (d, 1H, $J = 10.8$ Hz, H-6_{eq}), 2.48 (dd, 1H, $J = 10.8$ and 5.8 Hz, H-6_{ax}), 0.99 (s, 9H, $\text{C}(\text{CH}_3)_3$), 0.80 (s, 9H, $\text{C}(\text{CH}_3)_3$), 0.24 (s, 3H, SiCH₃), 0.22 (s, 3H, SiCH₃), 0.20 (s, 3H, SiCH₃), and 0.10 (s, 3H, SiCH₃) ppm. ^{13}C NMR (63 MHz, CDCl_3) δ 175.2 (C), 148.7 (C), 144.0 (C), 140.1 (C), 139.4 (C), 139.1 (C), 128.9 ($2 \times$ C), 124.4 (CH),

124.2 (CH), 123.8 (CH), 123.6 (CH), 123.1 (CH), 122.8 (CH), 122.6 (CH), 122.3 (CH), 121.9 (CH), 121.2 (CH), 74.7 (C), 74.6 (CH), 68.5 (CH₂), 67.4 (CH), 37.5 (CH₂), 25.7 ($\text{C}(\text{CH}_3)_3$), 25.5 ($\text{C}(\text{CH}_3)_3$), 18.1 ($\text{C}(\text{CH}_3)_3$), 18.0 ($\text{C}(\text{CH}_3)_3$), –3.3 (SiCH₃), –3.4 (SiCH₃), –4.4 (SiCH₃), and –4.5 (SiCH₃) ppm. IR (film): 1799 ($\text{C}=\text{O}$) cm^{-1} . MS (CI) m/z (%) 693 (MH^+). HRMS calcd for $\text{C}_{37}\text{H}_{49}\text{O}_5\text{S}_2\text{Si}_2$ (MH^+): 693.2560; found, 693.2563.

(**1R,4S,5R**)-**1,4-Di(tert-butylidemethylsilyloxy)-3-(5-methylbenzo[b]thiophen-2-yl)methoxycyclohexan-1,5-carbolactone (11d)** and (**1R,4S,5R**)-**1,4-Di(tert-butylidemethylsilyloxy)-3-(5-methylbenzo[b]thiophen-2-yl)methoxy-2-(5-methylbenzo[b]thiophen-2-yl)methylcyclhex-2-en-1,5-carbolactone (12d).** The reaction was carried out as for compounds **11c** and **12c** by using 200 mg of ketone **10** and 180 mg of 2-bromomethyl-5-methylbenzo[b]thiophene (**15d**) as starting materials. Yield: 62 mg (22%) of *O*-alkyl derivative **11d** and 99 mg (28%) of dialkyl derivative **12d**, both as light-yellow oils.

Data for 11d. $[\alpha]_D^{20} -120.6^\circ$ (c 1.0, CHCl_3). ^1H NMR (250 MHz, CDCl_3) δ 7.70 (d, 1H, $J = 8.5$ Hz, ArH), 7.54 (s, 1H, ArH), 7.17 (m, 2H, $2 \times$ ArH), 5.05 (s, 1H, H-2), 4.98 (d, 1H, $J = 12.0$ Hz, CHHAr), 4.92 (d, 1H, $J = 12.0$ Hz, CHHAr), 4.48 (dd, 1H, $J = 5.3$ and 3.5 Hz, H-5), 4.17 (d, 1H, $J = 3.5$ Hz, H-4), 2.46 (s, 3H, CH₃), 2.44–2.30 (m, 2H, H-6), 0.92 (s, 9H, $\text{C}(\text{CH}_3)_3$), 0.87 (s, 9H, $\text{C}(\text{CH}_3)_3$), 0.17 (s, 3H, SiCH₃), 0.12 (s, 3H, SiCH₃), 0.10 (s, 3H, SiCH₃), and 0.08 (s, 3H, SiCH₃) ppm. ^{13}C NMR (63 MHz, CDCl_3) δ 176.1 (C), 153.3 (C), 139.4 (C), 138.9 (C), 137.4 (C), 134.0 (C), 126.3 (CH), 123.6 (CH), 123.0 (CH), 122.0 (CH), 105.2 (CH), 75.3 (CH), 73.7 (C), 67.4 (CH), 65.2 (OCH₂), 38.0 (CH₂), 25.7 ($\text{C}(\text{CH}_3)_3$), 25.6 ($\text{C}(\text{CH}_3)_3$), 21.3 (CH₃), 18.1 ($\text{C}(\text{CH}_3)_3$), 18.0 ($\text{C}(\text{CH}_3)_3$), –3.1 ($2 \times \text{SiCH}_3$), –4.4 (SiCH₃), and –5.2 (SiCH₃) ppm. IR (film): 1801 ($\text{C}=\text{O}$) cm^{-1} . MS (CI) m/z (%) 561 (MH^+). HRMS calcd for $\text{C}_{29}\text{H}_{45}\text{O}_5\text{SSi}_2$ (MH^+): 561.2526; found, 561.2530.

Data for 12d. $[\alpha]_D^{20} -75.4^\circ$ (c 1.3, CHCl_3). ^1H NMR (250 MHz, CDCl_3) δ 7.65 (d, 1H, $J = 8.0$ Hz, ArH), 7.59 (d, 1H, $J = 8.0$ Hz, ArH), 7.45 (s, 1H, ArH), 7.37 (s, 1H, ArH), 7.13 (d, 1H, $J = 8.3$ Hz, ArH), 7.05 (d, 1H, $J = 8.3$ Hz, ArH), 6.95 (s, 1H, ArH), 6.87 (s, 1H, ArH), 5.02 (s, 2H, CH₂O), 4.57 (d, 1H, $J = 5.8$ and 3.3 Hz, H-5), 4.46 (d, 1H, $J = 3.3$ Hz, H-4), 3.93 (d, 1H, $J = 15.5$ Hz, CHHAr), 3.79 (d, 1H, $J = 15.5$ Hz, CHHAr), 4.17 (d, 1H, $J = 3.5$ Hz, H-4), 2.56 (d, 1H, $J = 10.8$ Hz, H-6_{eq}), 2.45 (m, 1H, H-6_{ax}), 2.44 (s, 3H, CH₃), 2.42 (s, 3H, CH₃), 0.96 (s, 9H, $\text{C}(\text{CH}_3)_3$), 0.78 (s, 9H, $\text{C}(\text{CH}_3)_3$), 0.21 (s, 3H, SiCH₃), 0.19 (s, 3H, SiCH₃), 0.16 (s, 3H, SiCH₃), and 0.07 (s, 3H, SiCH₃) ppm. ^{13}C NMR (63 MHz, CDCl_3) δ 175.2 (C), 148.6 (C), 144.0 (C), 140.4 (C), 139.8 (C), 139.5 (C), 137.3 (C), 136.5 (C), 133.9 (C), 133.3 (C), 129.0 (C), 126.1 (CH), 124.8 (CH), 123.6 (CH), 122.7 (CH), 122.6 (CH), 121.9 (CH), 121.5 (CH), 121.0 (CH), 74.7 (C), 74.6 (CH), 68.5 ($2 \times \text{CH}_2$), 67.4 (CH), 37.5 (CH₂), 25.7 ($\text{C}(\text{CH}_3)_3$), 25.5 ($\text{C}(\text{CH}_3)_3$), 21.4 (CH₃), 21.3 (CH₃), 18.1 ($\text{C}(\text{CH}_3)_3$), 18.0 ($\text{C}(\text{CH}_3)_3$), –3.3 (SiCH₃), –3.4 (SiCH₃), and –4.5 ($2 \times \text{SiCH}_3$) ppm. IR (film): 1799 ($\text{C}=\text{O}$) cm^{-1} . MS (CI) m/z (%) 721 (MH^+). HRMS calcd for $\text{C}_{39}\text{H}_{53}\text{O}_5\text{S}_2\text{Si}_2$ (MH^+): 721.2873; found, 721.2878.

(**1R,4S,5R**)-**1,4-Dihydroxy-3-(thien-3-yl)methoxycyclohex-2-en-1,5-carbolactone (13a).** A stirred solution of silyl ether **11a** (65 mg, 0.13 mmol) in dry THF (1.9 mL) was treated with tetrabutylammonium fluoride (0.29 mL, 0.29 mmol, ~1.0 M in THF). After 1 h, ethyl acetate and water were added. The organic layer was separated, and the aqueous phase was extracted with ethyl acetate ($\times 3$). All the combined organic extracts were dried (anhydrous Na_2SO_4), filtered, and concentrated under reduced pressure. The obtained residue was purified by flash chromatography, eluting with ethyl acetate–hexane (50:50) to afford 30 mg (86%) of diol **13a** as a white foam. $[\alpha]_D^{20} -189^\circ$ (c 1.5, MeOH). ^1H NMR (300 MHz, CD_3OD) δ 7.40 (dd, 1H, $J = 5.1$ and 0.9 Hz, ArH), 7.12 (d, 1H, $J = 2.7$ Hz, ArH), 6.99 (dd, 1H, $J = 5.1$ and 3.6 Hz, ArH), 5.15 (s, 1H, H-2), 4.99 (d, 1H, $J = 12.3$ Hz, CHHAr), 4.93 (d, 1H, $J = 12.3$ Hz, CHHAr), 4.61 (m, 1H, H-5), 4.08 (d, 1H, $J = 3.3$ Hz, H-4), and 2.32 (m, 2H, H-6) ppm. ^{13}C NMR (75 MHz,

CD_3OD) δ 179.2 (C), 155.3 (C), 146.0 (C), 139.6 (CH), 128.6 (CH), 127.7 (CH), 127.5 (CH), 127.5 (CH), 105.1 (CH), 76.9 (CH), 72.9 (C), 67.6 (CH_2), 65.5 (CH), and 38.3 (CH_2) ppm. IR (KBr): 3463 (O—H) and 1774 (C=O) cm^{-1} . MS (CI) m/z (%) 269 (MH $^+$). HRMS calcd for $\text{C}_{12}\text{H}_{13}\text{O}_5\text{S}$ (MH $^+$): 269.0484; found, 269.0480.

Sodium (1*R*,4*S*,5*R*)-1,4-Dihydroxy-3-(thien-3-yl)methoxycyclohex-2-en-1-carboxylate (9a). A solution of the lactone **13a** (29 mg, 0.11 mmol) in THF (1.0 mL) and aqueous sodium hydroxide (215 μL , 0.11 mmol, 0.5M) was stirred at room temperature for 15 min. Water was added, and THF was removed under reduced pressure. The resultant aqueous solution was washed with diethyl ether ($\times 2$), and the aqueous extract was liophilized to afford derivative **9a** (33 mg, 97%) as a beige solid. Mp: 125–128 $^\circ\text{C}$. $[\alpha]_D^{20}$ –31° (c 1.2, H₂O). ¹H NMR (300 MHz, D₂O) δ 7.48 (br d, 1H, J = 5.1 Hz, ArH), 7.19 (d, 1H, J = 3.0 Hz, ArH), 7.07 (dd, 1H, J = 5.1 and 3.6 Hz, ArH), 5.06 (d, 1H, J = 12.0 Hz, CHHAr), 4.99 (d, 1H, J = 12.0 Hz, CHHAr), 4.97 (s, 1H, H-2), 4.05 (d, 1H, J = 7.5 Hz, H-4), 3.96 (m, 1H, H-5), 2.08 (dd, 1H, J = 13.5 and 10.2 Hz, H-6_{ax}), and 2.00 (dd, 1H, J = 13.5 and 4.5 Hz, H-6_{eq}) ppm. ¹³C NMR (75 MHz, D₂O) δ 184.5 (C), 158.3 (C), 141.4 (C), 131.1 (CH), 130.3 (CH), 130.2 (CH), 103.7 (CH), 76.9 (C), 75.0 (CH), 72.6 (CH), 67.3 (CH₂), and 41.9 (CH₂) ppm. IR (KBr): 3419 (O—H), 1653 and 1601 (C=O) cm^{-1} . MS (ESI) m/z (%) 331 (MNa $^+$). HRMS calcd for $\text{C}_{12}\text{H}_{13}\text{O}_6\text{SNa}_2$ (MH $^+$): 331.0223; found, 331.0219.

(1*R*,4*S*,5*R*)-3-(Benzo[b]thiophen-5-yl)methoxy-1,4-dihydroxy-cyclohex-2-en-1,5-carbolactone (13b). The same experimental procedure as for compound **13a** was used by using silyl ether **11b** (173 mg, 0.32 mmol) as starting material and tetrabutylammonium fluoride (0.70 mL, 0.70 mmol) and THF (4.5 mL). Yield: 94 mg (92%). White solid. Mp: 177–179 $^\circ\text{C}$. $[\alpha]_D^{20}$ –153° (c 1.0, MeOH). ¹H NMR (250 MHz, CD₃OD) δ 7.81 (m, 2H, 2 \times ArH), 7.51 (d, 1H, J = 5.5 Hz, ArH), 7.31 (m, 2H, 2 \times ArH), 5.08 (s, 1H, H-2), 4.84 (s, 2H, CH₂O), 4.57 (m, 1H, H-5), 4.08 (d, 1H, J = 3.2 Hz, H-4), and 2.26 (m, 2H, H-6) ppm. ¹³C NMR (63 MHz, CD₃OD) δ 179.2 (C), 155.6 (C), 141.2 (C), 140.7 (C), 133.8 (C), 128.1 (CH), 125.1 (CH), 124.8 (CH), 123.8 (CH), 123.3 (CH), 104.9 (CH), 76.9 (CH), 72.9 (C), 70.9 (CH₂), 67.7 (CH), and 38.3 (CH₂) ppm. IR (film): 3431 (O—H) and 1763 (C=O) cm^{-1} . MS (CI) m/z (%) 319 (MH $^+$). HRMS calcd for $\text{C}_{16}\text{H}_{15}\text{O}_5\text{S}$ (MH $^+$): 319.0640; found, 319.0640.

Sodium (1*R*,4*S*,5*R*)-1,4,5-Trihydroxy-3-[(benzo[b]thiophen-5-yl)methoxy]cyclohex-2-en-1-carboxylate (9b). The experimental procedure used was the same as for compound **9a** using 20 mg (0.06 mmol) of lactone **13b**, 125 μL of NaOH, and 0.6 mL of THF. Yield = 21 mg (98%). White solid. Mp: 157–160 $^\circ\text{C}$ (dec). $[\alpha]_D^{20}$ –26° (c 1.4, H₂O). ¹H NMR (250 MHz, D₂O) δ 7.99 (d, 1H, J = 8.5 Hz, ArH), 7.92 (s, 1H, ArH), 7.63 (d, 1H, J = 5.2 Hz, ArH), 7.45 (s, 1H, ArH), 7.42 (m, 1H, ArH), 4.94 (m, 3H, CH₂O + H-2), 4.09 (d, 1H, J = 7.2 Hz, H-4), 3.98 (m, 1H, H-5), 2.11 (dd, 1H, J = 13.5 and 10.2 Hz, H-6_{ax}), and 2.00 (dd, 1H, J = 13.5 and 4.2 Hz, H-6_{eq}) ppm. ¹³C NMR (63 MHz, D₂O) δ 182.1 (C), 156.3 (C), 140.3 (C), 139.9 (C), 133.3 (C), 128.5 (CH), 125.0 (CH), 124.5 (CH), 123.8 (CH), 123.4 (CH), 101.1 (CH), 74.4 (C), 72.6 (CH), 70.4 (CH₂), 70.2 (CH), and 39.5 (CH₂) ppm. IR (KBr): 3419 (O—H), 1655 and 1597 (C=O) cm^{-1} . MS (ESI) m/z (%) 359 (MH $^+$). HRMS calcd for $\text{C}_{16}\text{H}_{16}\text{O}_6\text{SNa}$ (MH $^+$): 359.0560; found, 359.0560.

(1*R*,4*S*,5*R*)-1,4-Dihydroxy-3-(benzo[b]thiophen-2-yl)methoxycyclohexan-1,5-carbolactone (13c). The same experimental procedure as for compound **13a** was used by using silyl ether **11c** (42 mg, 0.077 mmol) as starting material and tetrabutylammonium fluoride (0.20 mL, 0.20 mmol) and THF (1.1 mL). Yield: 24 mg (99%). Beige solid. $[\alpha]_D^{20}$ –151.2° (c 1.1, MeOH). ¹H NMR (250 MHz, CD₃OD) δ 7.77 (m, 1H, ArH), 7.70 (m, 1H, ArH), 7.32–7.21 (m, 3H, 3 \times ArH), 5.13 (s, 1H, H-2), 5.02 (br s, 2H, CH₂O), 4.57 (m, 1H, H-5), 4.07 (d, 1H, J = 3.3 Hz, H-4), and 2.27 (m, 2H, H-6) ppm. ¹³C NMR (63 MHz, CD₃OD) δ 179.2 (C), 155.3 (C), 141.6 (C), 140.8 (C), 140.8 (C), 125.7 (CH), 125.5

(CH), 124.8 (CH), 124.6 (CH), 123.3 (CH), 105.4 (CH), 77.0 (CH), 73.0 (C), 67.6 (CH), 66.3 (CH₂), and 38.3 (CH₂) ppm. IR (KBr): 3390 (O—H) and 1765 (C=O) cm^{-1} . MS (ESI) m/z (%) 319 (MH $^+$). HRMS calcd for $\text{C}_{16}\text{H}_{15}\text{O}_5\text{S}$ (MH $^+$): 319.0635; found, 319.0634.

Sodium (1*R*,4*S*,5*R*)-1,4,5-Trihydroxy-3-(benzo[b]thiophen-2-yl)methoxycyclohexan-1-carboxylate (9c). The experimental procedure used was the same as for compound **9a** using 28 mg (0.09 mmol) of lactone **13c**, 176 μL of NaOH, and 0.8 mL of THF. Yield = 31 mg (98%). Beige solid. $[\alpha]_D^{20}$ –52.0° (c 1.3, MeOH). ¹H NMR (250 MHz, CD₃OD) δ 7.74 (m, 1H, ArH), 7.68 (m, 1H, ArH), 7.24 (m, 3H, 3 \times ArH), 5.01 (d, 1H, J = 12.5 Hz, CHHO), 4.94 (d, 1H, J = 12.5 Hz, CHHO), 4.82 (s, 1H, H-2), 3.87 (m, 2H, H-5 + H-4), and 2.05 (m, 2H, CH₂-6) ppm. ¹³C NMR (63 MHz, CD₃OD) δ 182.1 (C), 157.1 (C), 141.6 (2 \times C), 140.9 (C), 125.5 (CH), 125.4 (CH), 124.7 (CH), 124.1 (CH), 123.3 (CH), 103.6 (CH), 74.7 (C), 72.4 (CH), 71.6 (CH), 65.9 (OCH₂), and 37.4 (CH₂) ppm. IR (KBr): 3435 (O—H), 1664 (C=O), 1610 (C=O), and 1585 (C=O) cm^{-1} . MS (ESI) m/z (%) 359 (MH $^+$). HRMS calcd for $\text{C}_{16}\text{H}_{16}\text{O}_6\text{SNa}$ (MH $^+$): 359.0560; found, 359.0560.

(1*R*,4*S*,5*R*)-1,4-Dihydroxy-3-(5-methylbenzo[b]thiophen-2-yl)methoxycyclohexan-1,5-carbolactone (13d). The same experimental procedure as for compound **13a** was used by using silyl ether **11d** (72 mg, 0.13 mmol) as starting material and tetrabutylammonium fluoride (0.34 mL, 0.34 mmol) and THF (1.9 mL). Yield: 34 mg (79%). Beige solid. $[\alpha]_D^{20}$ –135.1° (c 1.4, acetone). ¹H NMR (250 MHz, CD₃OD) δ 7.63 (d, 1H, J = 8.3 Hz, ArH), 7.50 (m, 1H, ArH), 7.21 (m, 1H, ArH), 7.10 (m, 1H, ArH), 5.14 (s, 1H, H-2), 5.00 (br s, 2H, OCH₂), 4.60 (m, 1H, H-5), 4.08 (d, 1H, J = 3.3 Hz, H-4), 2.38 (s, 3H, CH₃), and 2.28 (m, 2H, CH₂-6) ppm. ¹³C NMR (63 MHz, CDCl₃) δ 179.2 (C), 155.3 (C), 141.1 (C), 140.8 (C), 138.8 (C), 135.3 (C), 127.3 (CH), 124.7 (CH), 124.4 (CH), 123.0 (CH), 105.4 (CH), 77.0 (CH), 73.0 (C), 67.6 (CH), 66.4 (OCH₂), 38.4 (CH₂), and 21.4 (CH₃) ppm. IR (KBr): 3444 (O—H), 3377 (O—H), and 1765 (C=O) cm^{-1} . MS (CI) m/z (%) 333 (MH $^+$). HRMS calcd for $\text{C}_{17}\text{H}_{17}\text{O}_5\text{S}$ (MH $^+$): 333.0797; found, 333.0786.

Sodium (1*R*,4*S*,5*R*)-1,4,5-Trihydroxy-3-(5-methylbenzo[b]thiophen-2-yl)methoxycyclohexan-1-carboxylate (9d). The same experimental procedure as for compound **9a** was used by using lactone **13d** (21 mg, 0.063 mmol) as starting material and THF (0.6 mL) and NaOH (126 μL). Yield: 22 mg (95%). Beige solid. $[\alpha]_D^{20}$ –41.9° (c 1.5, MeOH). ¹H NMR (250 MHz, CD₃OD) δ 7.63 (d, 1H, J = 8.3 Hz, H-4'), 7.50 (br s, 1H, H-7'), 7.21 (s, 1H, H-3'), 7.09 (dd, 1H, J = 8.3 and 1.0 Hz, H-5'), 5.01 (d, 1H, J = 12.3 Hz, CHH), 4.94 (d, 1H, J = 12.3 Hz, CHH), 4.84 (s, 1H, H-2), 3.88 (m, 2H, H-5 + H-4), 2.38 (s, 3H, CH₃), and 2.06 (m, 2H, CH₂-6) ppm. ¹³C NMR (63 MHz, CD₃OD) δ 182.1 (C), 157.2 (C), 141.7 (C), 141.3 (C), 138.9 (C), 135.2 (C), 127.1 (CH), 124.6 (CH), 123.9 (CH), 122.9 (CH), 103.5 (CH), 74.7 (C), 72.4 (CH), 71.6 (CH), 66.0 (OCH₂), 37.4 (CH₂), and 21.5 (CH₃) ppm. IR (KBr): 3435 (O—H), 1649 and 1618 (C=O) cm^{-1} . MS (ESI) m/z (%) 373 (MH $^+$). HRMS calcd for $\text{C}_{17}\text{H}_{18}\text{O}_6\text{SNa}$ (MH $^+$): 373.0716; found, 373.0729.

Dehydroquinase Assays. *Helicobacter pylori* type II dehydroquinase was expressed and purified as we described previously.²² A concentrated solution of *H. pylori* dehydroquinase (6.4 mg mL⁻¹) was stored in potassium phosphate buffer (50 mM, pH 7.2), DTT (1 mM), and NaCl (150 mM). When required for assays, aliquots of the enzyme stocks were diluted into water and buffer and stored on ice. Dehydroquinase was assayed in the forward direction by monitoring the increase in absorbance at 234 nm in the UV spectrum because of the absorbance of the enone–carboxylate chromophore of 3-dehydrosikimic acid (**6**) (ϵ = 12 000 M⁻¹ cm⁻¹). Standard assay conditions for DHQ2-Hp were pH 7.0 at 25 °C in Tris-HCl (50 mM). Each assay was initiated by addition of the substrate. Solutions of 3-dehydroquinic acid (**4**) were calibrated by equilibration with DHQ2 and measurement of the change in the UV absorbance at 234 nm due

to the formation of the enone–carboxylate chromophore of 3-dehydroshikimic acid (**6**). The K_i values of acids **9** against DHQ2-Hp were obtained from Dixon plots ($1/v$ vs $[I]$)²⁴ of assay data. The initial rates at fixed enzyme and substrate concentrations (0.25–1.4 K_m) were measured in the absence and in the presence of various inhibitor concentrations. A standard inhibition assay consists of (1) incubation of 10 μL of enzyme solution (in buffer) and the tested inhibitor (in water) in 50 mM Tris-HCl, pH 7, at 25 °C for 10 min, (2) addition of substrate (in water) and after 1 min measurement of the initial rate at 234 nm at 25 °C.

Crystallization and Structure Determination. *H. pylori* type II dehydroquinase was concentrated to 20 mg mL^{-1} in 50 mM Tris-HCl, pH 7.5, 1 mM 2-mercaptopropanoic acid, 1 mM ethylenediaminetetraacetic acid, and 200 mM sodium chloride. Compound **9d** was dissolved at 0.25 M in methanol and added at a ratio of 1:20 (v/v) to the protein solution to give a solution of approximately 10 equiv of **9d** per protein monomer. Diamond-shaped crystals of up to 0.3 mm × 0.2 mm were obtained after 3 weeks of sitting drop vapor diffusion of 2.5 μL of protein/inhibitor solution mixed with 2.5 μL of reservoir solution against 0.15 mL reservoirs containing 26% (w/v) polyethylene-glycol 4000 and 0.1 M 2-(*N*-morpholino)ethanesulfonic acid–sodium hydroxide, pH 5.0. After harvesting, crystals were sequentially transferred to solutions containing 35% and 45% (w/v) polyethylene glycol 4000 in 0.1 M 2-(*N*-morpholino)ethanesulfonic acid–sodium hydroxide, pH 5.0, and flash-frozen in liquid nitrogen. Data were collected at the EMBL X11 beamline at the DORIS storage ring (DESY, Hamburg, Germany) from a crystal maintained at 100 K. Crystallographic data were integrated using MOSFLM²⁷ and further processed using SCALA²⁸ and other programs of the CCP4 software suite.²⁹ The structure was solved by molecular replacement, using the program PHASER³⁰ and PDB entry 2C4V.²⁵ Reflections for calculating R_{free} ³¹ were selected in thin resolution shells. Model building was done with COOT³² and refinement with REFMAC.³³ Validation was performed with MOLPROBITY.³⁴ For data, refinement, and model statistics, see Table 2. Coordinates and structure factors are available from the Protein Data Bank with accession code 2WKS. Structure figures were prepared using PYMOL³⁵ and VMD.³⁶

Acknowledgment. We thank Patricia Ferraces-Casais for excellent technical assistance and EMBL-Hamburg scientists Paul Tucker and Santosh Panjikar for help with synchrotron data collection. This work was supported by the Spanish Ministry of Science and Innovation (under Projects SAF2007-63533 to C.G.B., BFU2005-02974/BMC and BFU2008-01588/BMC to M.J.v.R.), CSIC (Grant 488IE7 to M.J.v.R.), and the Xunta de Galicia (Grants PGIDT07PXIB209080PR and GRC2006/132 to C.G.B.). V.F.V.P., J.M.O., L.T., and P.G.-C. thank the Portuguese Fundação para a Ciência e a Tecnologia for a FCT fellowship, the Xunta de Galicia for a “Angeles Alvariño” contract, and the Spanish Ministry of Science and Innovation for FPU fellowships, respectively. Data collection at EMBL/DESY was supported by the European Community FP6 Research Infrastructure Action “Structuring the European Research Area”, Contract No. RII3/CT/2004/5060008.

Supporting Information Available: ^1H NMR, ^{13}C NMR, and DEPT spectra, Dixon plots for compounds **9**, a table of close contacts between ligand **9b** and DHQ2-Hp, and a figure with the electron density for inhibitor **9d** in crystal structure with the final $2F_o - F_c$ map contoured at 1σ . This material is available free of charge via the Internet at <http://pubs.acs.org>.

References

- (a) Arias, C. A.; Murray, B. E. Antibiotic-resistant bugs in the 21st century. A clinical super-challenge. *N. Engl. J. Med.* **2009**, *360*, 439–443. (b) Jayaraman, R. Bacterial persistence: some new insights into an old phenomenon. *J. Biosci.* **2008**, *33*, 795–805.
- (a) Giamarellou, H. Treatment options for multidrug-resistant bacteria. *Expert Rev. Anti-Infect. Ther.* **2006**, *4*, 601–618. (b) Appelbaum, P. C.; Jacobs, M. R. Recently approved and investigational antibiotics for treatment of severe infections caused by Gram-positive bacteria. *Curr. Opin. Microbiol.* **2005**, *8*, 510–517. (c) Okeke, I. N.; Klugman, K. P.; Bhutta, Z. A.; Duse, A. G.; Jenkins, P.; O'Brien, T. F.; Pablos-Mendez, A.; Laxminarayan, R. Antimicrobial resistance in developing countries. Part II: Strategies for containment. *Lancet Infect. Dis.* **2005**, *5*, 568–580.
- Graham, D. Y.; Shiotani, A. New concepts of resistance in the treatment of *Helicobacter pylori* infections. *Nat. Clin. Pract. Gastroenterol. Hepatol.* **2008**, *5*, 321–331.
- Duck, W. M.; Sobel, J.; Pruckler, J. M.; Song, Q.; Swerdlow, D.; Friedman, C.; Sulka, A.; Swaminathan, B.; Taylor, T.; Hoekstra, M.; Griffin, P.; Smoot, D.; Peek, R.; Metz, D. C.; Bloom, P. B.; Goldschmid, S.; Parsonnet, J.; Triadafilopoulos, G.; Pérez-Pérez, G. I.; Vakil, N.; Ernst, P.; Czinn, S.; Dunne, D.; Gold, B. D. Antimicrobial resistance incidence and risk factors among *Helicobacter pylori*-infected persons, United States. *Emerg. Infect. Dis.* **2004**, *10*, 1088–1094.
- Megraud, F. *H. pylori* antibiotic resistance: prevalence, importance, and advances in testing. *Gut* **2004**, *53*, 1374–1384.
- Bruce, M. G.; Bruden, D. L.; McMahon, B. J.; Hennessy, T. W.; Reasonover, A.; Morris, J.; Hurlburt, D. A.; Peters, H.; Sacco, F.; Martínez, P.; Swenson, M.; Berg, D. E.; Parks, D.; Parkinson, A. J. Alaska sentinel surveillance for antimicrobial resistance in *Helicobacter pylori* isolates from Alaska native persons, 1999–2003. *Helicobacter* **2006**, *11*, 581–588.
- Hatakeyama, M. *Helicobacter pylori* and gastric carcinogenesis. *J. Gastroenterol.* **2009**, *44*, 239–248.
- Gonzalez-Bello, C.; Castedo, L. Progress in type II dehydroquinase inhibitors: From concept to practice. *Med. Res. Rev.* **2007**, *27*, 177–208.
- Haslam, E. *The Shikimate Pathway*; Wiley: New York, 1974.
- Abell, A. Enzymology and Molecular Biology of the Shikimate Pathway. In *Comprehensive Natural Products Chemistry*; Sankawa, U., Ed.; Elsevier Science Ltd.: Oxford, U.K., 1999; pp 573–607.
- (a) Roberts, F.; Roberts, C. W.; Johnson, J. J.; Kyle, D. E.; Krell, T.; Coggins, J. R.; Coombs, G. H.; Milhous, W. K.; Tzipori, S.; Ferguson, D. J.; Chakrabarti, D.; McLeod, R. Evidence for the shikimate pathway in apicomplexan parasites. *Nature* **1998**, *393*, 801–805. (b) Keeling, P. J.; Palmer, J. D.; Donald, R. G.; Roos, D. S.; Waller, R. F.; McFadden, G. I. Shikimate pathway in apicomplexan parasites. *Nature* **1999**, *397*, 219–220. (c) Campbell, S. A.; Richards, T. A.; Mui, E. J.; Samuel, B. U.; Coggins, J. R.; McLeod, R.; Roberts, C. W. A complete shikimate pathway in *Toxoplasma gondii*: an ancient eukaryotic innovation. *Int. J. Parasitol.* **2004**, *34*, 5–13. (d) Roberts, C. W.; Roberts, F.; Lyons, R. E.; Kirisits, M. J.; Mui, E. J.; Finnerty, J.; Johnson, J. J.; Ferguson, D. J.; Coggins, J. R.; Krell, T.; Coombs, G. H.; Milhous, W. K.; Kyle, D. E.; Tzipori, S.; Barnwell, J.; Dame, J. B.; Carlton, J.; McLeod, R. The shikimate pathway and its branches in apicomplexan parasites. *J. Infect. Dis.* **2002**, *185* (Suppl. 1), S25–S36. (e) McConkey, G. A.; Pinney, J. W.; Westhead, D. R.; Plueckhahn, K.; Fitzpatrick, T. B.; Macheroux, P.; Kappes, B. Annotating the *Plasmodium* genome and the enigma of the shikimate pathway. *Trends Parasitol.* **2004**, *20*, 60–65.
- (a) Salama, N. R.; Shepherd, B.; Falkow, S. Global transposon mutagenesis and essential gene analysis of *Helicobacter pylori*. *J. Bacteriol.* **2004**, *186*, 7926–7935. (b) Sassevi, C. M.; Boyd, D. H.; Rubin, E. J. Genes required for mycobacterial growth defined by high density mutagenesis. *Mol. Microb.* **2003**, *48*, 77–84. (c) de Berardinis, V.; Vallenet, D.; Castelli, V.; Besnard, M.; Pinet, A.; Cruaud, C.; Samair, S.; Lechaplais, C.; Gyapay, G.; Richez, C.; Durot, M.; Kreimeyer, A.; Le Févre, F.; Schächter, V.; Pezo, V.; Döring, V.; Scarpelli, C.; Médigue, C.; Cohen, G. N.; Marlière, P.; Salanoubat, M.; Weissenbach, J. A complete collection of single-gene deletion mutants of *Acinetobacter baylyi* ADP1. *Mol. Syst. Biol.* **2008**, *4*, 1–15.
- For a database of essential bacterial genes, see the following: (a) www.essentialgene.org. (b) Zhang, R.; Lin, Y. DEG 5.0, a database of essential genes in both prokaryotes and eukaryotes. *Nucleic Acids Res.* **2009**, *37*, D455–D458. (c) Zhang, R.; Ou, H.-Y.; Zhang, C.-T. DEG: a database of essential genes. *Nucleic Acids Res.* **2004**, *32*, D271–D272.
- Kleanthous, C. K.; Deka, R.; Davis, K.; Kelly, S. M.; Cooper, A.; Harding, S. E.; Price, N. C.; Hawkins, A. R.; Coggins, J. R. A comparison of the enzymological and biophysical properties of two distinct classes of dehydroquinase enzymes. *Biochem. J.* **1992**, *282*, 687–695.
- Shneier, A.; Harris, J.; Kleanthous, C.; Coggins, J. R.; Hawkins, A. R.; Abell, C. Evidence for opposite stereochemical courses for the

- reactions catalyzed by type I and type II dehydroquinases. *Bioorg. Med. Chem. Lett.* **1993**, *3*, 1399–1402.
- (16) (a) Duncan, K.; Chaudhuri, S.; Campbell, M. S.; Coggins, J. R. The overexpression and complete amino acid sequence of *Escherichia coli* 3-dehydroquinase. *Biochem. J.* **1986**, *238*, 475–483. (b) Servos, S.; Chatfield, S.; Hone, D.; Levine, M.; Dimitriadis, G.; Pickard, D.; Dougan, G.; Fairweather, N.; Charles, I. G. Molecular cloning and characterization of the aroD gene encoding 3-dehydroquinase from *Salmonella typhi*. *J. Gen. Microbiol.* **1991**, *137*, 147–152.
 - (17) (a) Moore, J. D.; Lamb, H. K.; Garbe, T.; Servos, S.; Dougan, G.; Charles, I. G.; Hawkins, A. R. Inducible overproduction of the *Aspergillus nidulans* pentafunctional AROM protein and the type-I and -II 3-dehydroquinases from *Salmonella typhi* and *Mycobacterium tuberculosis*. *Biochem. J.* **1992**, *287*, 173–181. (b) Garbe, T.; Servos, S.; Hawkins, A. R.; Dimitriadis, G.; Young, D.; Dougan, G.; Charles, I. The *Mycobacterium tuberculosis* shikimate pathway genes: evolutionary relationship between biosynthetic and catabolic 3-dehydroquinases. *Mol. Gen. Genet.* **1991**, *228*, 385–392. (c) Bottomley, J. R.; Clayton, C. L.; Chalk, P. A.; Kleanthous, C. Cloning, sequencing, expression, purification and preliminary characterization of a type II dehydroquinase from *Helicobacter pylori*. *Biochem. J.* **1996**, *319*, 559–565. (d) White, P. J.; Young, J.; Hunter, I. S.; Nimmo, H. G.; Coggins, J. R. The purification and characterization of 3-dehydroquinase from *Streptomyces coelicolor*. *Biochem. J.* **1990**, *265*, 735–738.
 - (18) (a) Roszak, A. W.; Robinson, D. A.; Krell, T.; Hunter, I. S.; Frederickson, M.; Abell, C.; Coggins, J. R.; Lapthorn, A. J. The structure and mechanism of the type II dehydroquinase from *Streptomyces coelicolor*. *Structure* **2002**, *10*, 493–503. (b) Harris, J.; González-Bello, C.; Kleanthous, C.; Coggins, J. R.; Hawkins, A. R.; Abell, C. Evidence from kinetic isotope studies for an enolate intermediate in the mechanism of type II dehydroquinases. *Biochem. J.* **1996**, *319*, 333–336.
 - (19) Krell, T.; Horsburgh, M. J.; Cooper, A.; Kelly, S. M.; Coggins, J. R. Localization of the active site of type II dehydroquinase. Identification of a common arginine-containing motif in the two classes of dehydroquinases. *J. Biol. Chem.* **1996**, *271*, 24492–24497.
 - (20) Krell, T.; Pitt, A. R.; Coggins, J. R. The use of electrospray mass spectrometry to identify an essential arginine residue in type II dehydroquinases. *FEBS Lett.* **1995**, *360*, 93–96.
 - (21) Payne, R. J.; Riboldi-Tunnicliffe, A. L.; Kerbarh, V. V. V.; Abell, A. D.; Lapthorn, A. J.; Abell, C. Design, synthesis, and structural studies on potent biaryl inhibitors of type II dehydroquinases. *ChemMedChem* **2007**, *2*, 1010–1013.
 - (22) Sánchez-Sixto, C.; Prazeres, V. F.; Castedo, L.; Suh, S. W.; Lamb, H.; Hawkins, A. R.; Cañada, F. J.; Jiménez-Barbero, J.; González-Bello, C. Competitive Inhibitors of *Helicobacter pylori* type II dehydroquinase: synthesis, biological evaluation, and NMR studies. *ChemMedChem* **2008**, *3*, 756–770.
 - (23) Sánchez-Sixto, C.; Prazeres, V. F. V.; Castedo, L.; Lamb, H.; Hawkins, A. R.; González-Bello, C. Structure-based design, synthesis and biological evaluation of inhibitors of *Mycobacterium tuberculosis* type II dehydroquinase. *J. Med. Chem.* **2005**, *48*, 4871–4881.
 - (24) (a) Dixon, M. The determination of enzyme inhibitor constants. *J. Am. Chem. Soc.* **1953**, *55*, 170–171. (b) *Enzymes and Their Inhibition, Drug Development*; Smith, H. J., Simons, C., Eds.; CRC Press: Boca Raton, FL, 2005; pp 156–161.
 - (25) Robinson, D. A.; Stewart, K. A.; Price, N. C.; Chalk, P. A.; Coggins, J. R.; Lapthorn, A. J. Crystal structures of *Helicobacter pylori* type II dehydroquinase inhibitor complexes: new directions for inhibitor design. *J. Med. Chem.* **2006**, *49*, 1282–1290.
 - (26) http://www.ccdc.cam.ac.uk/products/life_sciences/gold/.
 - (27) Leslie, A. G. The integration of macromolecular diffraction data. *Acta Crystallogr., Sect. D: Biol. Crystallogr.* **2006**, *62*, 48–57.
 - (28) Evans, P. Scaling and assessment of data quality. *Acta Crystallogr., Sect. D: Biol. Crystallogr.* **2006**, *62*, 72–82.
 - (29) Winn, M. D. An overview of the CCP4 project in protein crystallography: an example of a collaborative project. *J. Synchrotron Radiat.* **2003**, *10*, 23–25.
 - (30) McCoy, A. J.; Grosse-Kunstleve, R. W.; Adams, P. D.; Winn, M. D.; Storoni, L. C.; Read, R. J. Phaser crystallographic software. *J. Appl. Crystallogr.* **2007**, *40*, 658–674.
 - (31) Brunger, A. T. Free R value: cross-validation in crystallography. *Methods Enzymol.* **1997**, *277*, 366–396.
 - (32) Emsley, P.; Cowtan, K. Coot: model-building tools for molecular graphics. *Acta Crystallogr., Sect. D: Biol. Crystallogr.* **2004**, *60*, 2126–2132.
 - (33) Murshudov, G. N.; Vagin, A. A.; Dodson, E. J. Refinement of macromolecular structures by the maximum-likelihood method. *Acta Crystallogr., Sect. D: Biol. Crystallogr.* **1997**, *53*, 240–255.
 - (34) Davis, I. W.; Leaver-Fay, A.; Chen, V. B.; Block, J. N.; Kapral, G. J.; Wang, X.; Murray, L. W.; Arendall, W. B., 3rd; Snoeyink, J.; Richardson, J. S.; Richardson, D. C. MolProbity: all-atom contacts and structure validation for proteins and nucleic acids. *Nucleic Acids Res.* **2007**, *35*, W375–W383.
 - (35) DeLano, W. L. *The PyMOL Molecular Graphics System*; DeLano Scientific LLC, Palo Alto, CA, 2008; <http://www.pymol.org>.
 - (36) Theoretical and Computational Biophysics Group at the Beckman Institute, University of Illinois at Urbana—Champaign. <http://www.ks.uiuc.edu/>.